

# Optimization of the Deposition Conditions and Structural Characterization of $Y_1Ba_2Cu_3O_{7-x}$ Thin Superconducting Films.

J. Chrzanowski, S. Meng-Burany, W. B. Xing, A.E. Curzon, B. Heinrich and J.C. Irwin, *Department of Physics, Simon Fraser University, Burnaby, B. C., Canada V5A 1S6.*

R. A. Cragg, H. Zhou, F. Habib, V. Angus and A. A. Fife, *CTF Systems, Inc., 15-1750 McLean Ave., Port Coquitlam, B.C., Canada V3C 1M9.*

## ABSTRACT

Two series of  $Y_1Ba_2Cu_3O_z$  thin films deposited on (001)  $LaAlO_3$  single crystals by excimer laser ablation under two different protocols have been investigated. The research has yielded well defined deposition conditions in terms of oxygen partial pressure  $p(O_2)$  and substrate temperature of the deposition process  $T_h$ , for the growth of high quality epitaxial films of YBCO. The films grown under conditions close to optimal for both  $j_c$  and  $T_c$  exhibited  $T_c \geq 91$  K and  $j_c \geq 4 \times 10^6$  A/cm<sup>2</sup>, at 77 K. Close correlations between the structural quality of the film, the growth parameters ( $p(O_2)$ ,  $T_h$ ) and  $j_c$  and  $T_c$  have been found.

## 1. Introduction.

There are several technological difficulties which occur in the growth of high- $T_c$  films regardless of the deposition technique. These involve optimization of the oxygen partial pressure, the substrate temperature, the substrate surface preparation, the laser beam energy density, cooling procedure, etc. Moreover the deposition of superconducting oxides is further complicated because of the multielemental structure of the compounds and their sensitivity to film cation-composition [1] and oxygenation [2] which substantially influence both the superconducting properties and morphology of the film [1, 2]. These observations clearly manifest the importance of a precise and reliable control of the growth parameters of copper oxide superconducting films.

To investigate the many growth parameters the precise control of the oxygen pressure,  $p(O_2)$ , and substrate temperature,  $T_h$ , must be identified first. The aim of the present research was thus twofold: 1) Optimization of the deposition conditions for the growth of epitaxial films with the highest  $j_c$  and  $T_c$ , exhibiting simultaneously the best

morphology. 2) Structural characterization of the film and a search for correlations between the structural and superconducting properties of the film.

## 2. Experimental.

Thin films of YBCO were prepared by laser deposition using a YBCO target and pulsed excimer laser. The substrates used were LaAlO<sub>3</sub> (001) single crystals which possess a lattice spacing  $a = 3.79 \text{ \AA}$ , which is closely matched to the a-b plane spacing of YBCO. A Lambda Physik LPX 2051 excimer laser with  $\lambda = 248 \text{ nm}$  (KFr) operated at a repetition rate of 5-10 Hz, and at a fluence of  $1.5 \text{ J/cm}^2$  was used. The illuminated area was  $4 \times 2 \text{ mm}^2$ , and the laser was equipped with special electrodes to improve the beam profile uniformity. Two similar systems were used to obtain films fabricated under the two different protocols. In protocol 1 (film series 1), a constant temperature of the substrate heater was maintained ( $T_h = 820 \text{ }^\circ\text{C}$ ) while the oxygen partial pressure in the deposition chamber was variable ( $50 < p(\text{O}_2) < 300 \text{ mTorr}$ ). In protocol 2 (film series 2), a constant pressure of oxygen was maintained ( $p(\text{O}_2) = 200 \text{ mTorr}$ ), while the temperature of the heater was variable ( $740 < T_h < 820^\circ \text{ C}$ ).

For protocol 1 the target holder was a Kurt J. Lesker Co, Polygun system which holds up to six 2.5 cm diameter targets in a hexagonal carousel rotated under computer control synchronized with the laser firing. In protocol 2, a single YBCO target was rotated around the axis normal to the target face. In both systems the separation between the target and the substrate was the same;  $s = 5 \text{ cm}$ .

After deposition using either protocol the films were cooled slowly ( $5^\circ \text{ C/min}$ ) down to room temperature in 600 mTorr of oxygen. The resulting film thickness was  $3000 \text{ \AA}$ . The films were very smooth exhibiting a mirror-like appearance. Microscopic observations, however revealed the existence of numerous pinholes (of sub-micron size) which apparently did not affect  $j_c$  and  $T_c$  in the films.

Application of the two different deposition protocols enabled us to explore regions in the  $p(\text{O}_2)$  vs.  $1/T$  phase diagram of YBCO situated close to the YBCO stability line, Fig. 1, which according to previous reports [3-5] represent the most promising regime for the growth of high quality YBCO films.

To obtain the best conditions for the film growth in terms of the oxygen pressure and the substrate temperature during the film deposition, the phase diagrams  $p(\text{O}_2)$  versus  $1/T$  for YBCO by Bormann, Hammond and Noelting (B-H-N) [3,4] and by Beyers and Ahn [5] were used for a starting point in the studies presented in this paper. However, one

has to remember that the specific conditions for film growth may vary between different systems and methods of film deposition.

In Fig. 1 the continuous dark line denotes the most recent [5] thermodynamical stability line for tetragonal YBCO, while the discontinuous one represents a previous stability line [3,4] and is shown only for comparison. We will discuss our results with regard to the new stability line. The critical current density,  $j_c$ , and the critical temperature,  $T_c$ , were determined by an inductive method [6]. The width of the superconducting phase transition was  $\Delta T_c \sim 0.5K$ .

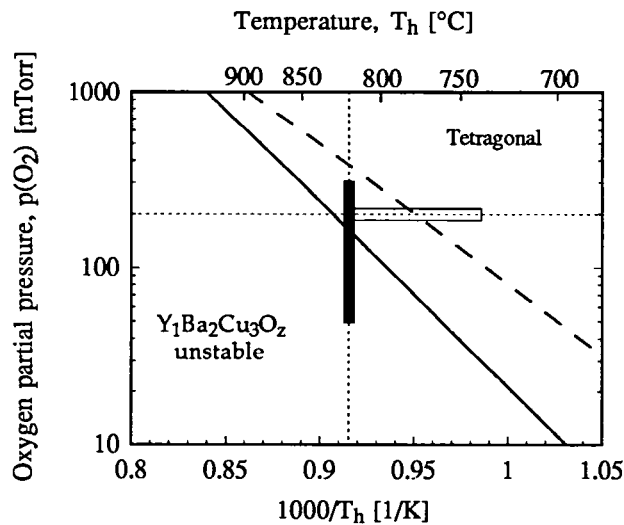


Fig. 1. Graph of oxygen partial pressure  $p(O_2)$  versus temperature  $T$  showing the critical stability line for tetragonal  $Y_1Ba_2Cu_3O_z$  ( $z = 6.0$ ), according to recent data (Ref. 5); continuous line. The old stability line published by Bormann, Hammond and Noelting (Ref. 3 and 4) is also shown for comparison as a broken line. The black and white areas denote the  $p$ - $T$  phase space where series 1 and 2 were grown, respectively.

### 3. Results and discussion.

#### 3.1. Optimization of the growth conditions.

The measurements of  $T_c$  and  $j_c$  as a function of the oxygen partial pressure  $p(O_2)$  and the substrate temperature  $T_h$  are presented in Figs. 2 and 3. It is interesting to note that while the critical temperature appears to be a monotonic function of  $p(O_2)$  and  $T_h$ , the critical current density  $j_c$  in the films in both series exhibits a distinct maximum as a function of  $p(O_2)$  or  $T_h$ . The highest  $T_c$  was 90 K in series 1 (variable oxygen pressure), and 92 K, in series 2 ( $p(O_2) = 200$  mTorr), while maxima of  $j_c$  were  $3.4$  and  $4.5 \times 10^6$  A/cm<sup>2</sup>, respectively. On average both parameters,  $T_c$  and  $j_c$ , were somewhat higher in series 2, though the differences in  $j_c$  remained practically within the limits of experimental

errors of  $j_c$  ( $\pm 10\%$ ). As can be seen in Figs. 2a and 3a, the critical temperature  $T_c$  was observed to rise with an increasing oxygen partial pressure  $p(O_2)$ , approaching a saturation value of 90 K for  $p(O_2) > 200$  mTorr. However when the substrate temperature  $T_h$  was increased from 740 to 820 °C, at  $p(O_2) = 200$  mTorr, a systematic decrease in  $T_c$  from 92 to  $\sim 88$  K was observed. In both film series  $p(O_2)$  and  $T_h$  moved in the phase diagram in the directions above and to the right of the stability line.

Figures 2 and 3 showed that the highest values of  $T_c$  and  $j_c$  do not occur under the same deposition conditions. Note that the highest values of  $j_c$  (Figures 2b and 3b) occur in the vicinity of the stability line of tetragonal YBCO where less perfect crystalline structure can be expected.

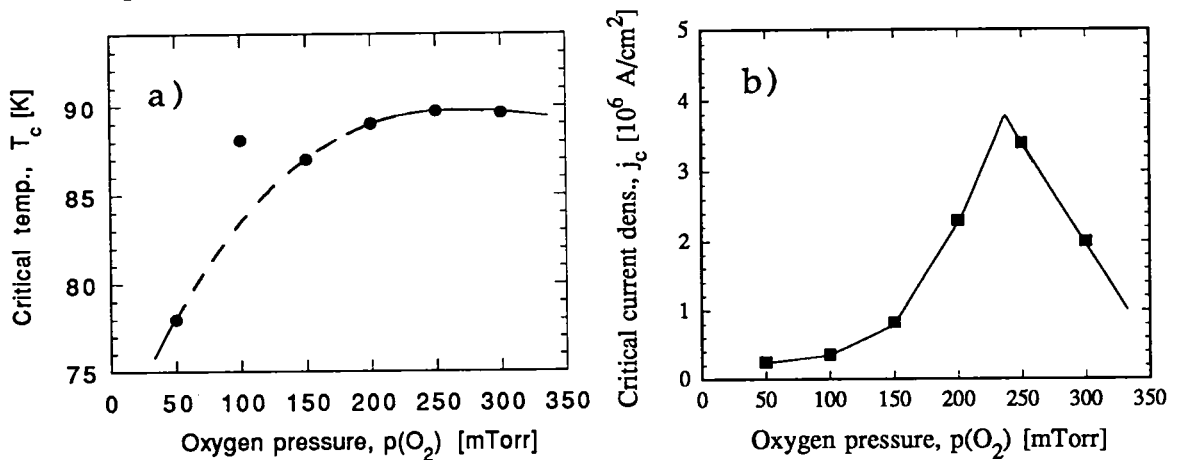


Fig. 2. Critical temperature  $T_c$  (a) and critical current density  $j_c$  (b) as functions of the oxygen pressure during film deposition (protocol 1).

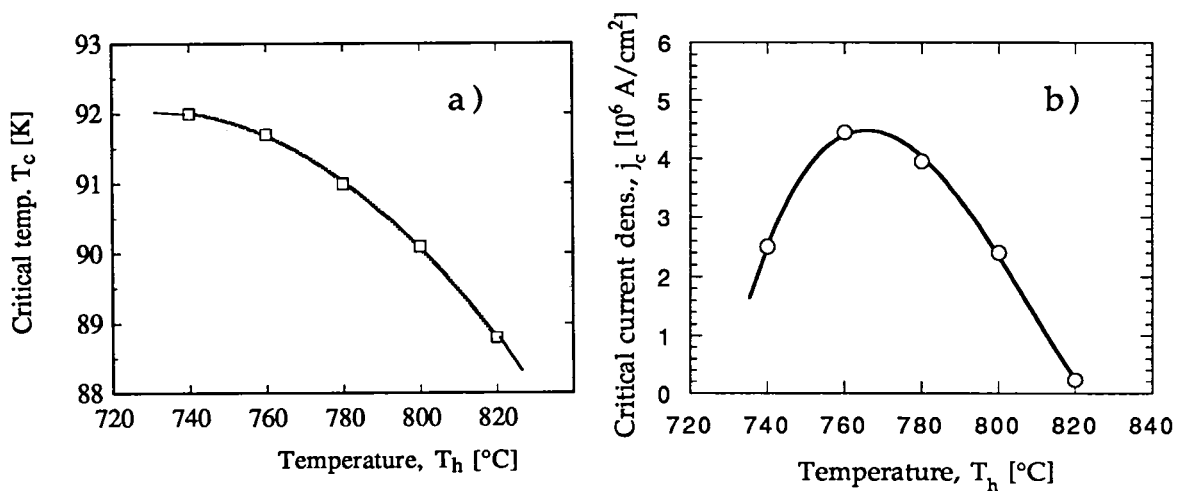


Fig. 3. Critical temperature  $T_c$  (a) and critical current density  $j_c$  (b) as functions of the film deposition temperature  $T_h$  (protocol 2).

### 3.2 Structural Characterization of Films.

Structural characterization of film series 1 and 2 have been carried out employing X-ray diffraction (XRD), scanning electron microscopy (SEM), energy dispersive analysis of X-rays (EDAX) and Raman spectroscopy.

A typical X-ray pattern of a YBCO film belonging to series 2 is presented in Fig. 4. It is evident that only  $(00\ell)$  Bragg reflections are present indicating a highly c-axis oriented texture. The  $(00\ell)$  lines behaved in a similar manner and therefore only the changes in the  $(005)$  line were used to characterize the films. The intensity ratio of the  $(005)$  X-ray peaks with respect to the background, for the films deposited under conditions close to optimal, was in excess of 2000. When the ratio of the count rate  $I(005)/\text{background}$  increased above  $\sim 1000$ , it was possible to observe the splitting of the  $K\alpha_1$  and  $K\alpha_2$  Copper X-ray doublet. The peak half-width for an individual  $K\alpha$ -line reflection was observed to be  $\Delta(2\theta) = 0.07^\circ$ , which indicates excellent crystallinity in the film. A corroboration of the structural perfection was provided also by measurements of the mosaic spread and electron channeling patterns. The in-plane epitaxy, was also investigated by using Raman spectroscopy [7]. The Raman measurements showed that the degree of the epitaxial growth occurred over 82 to 95% of the sampled area.

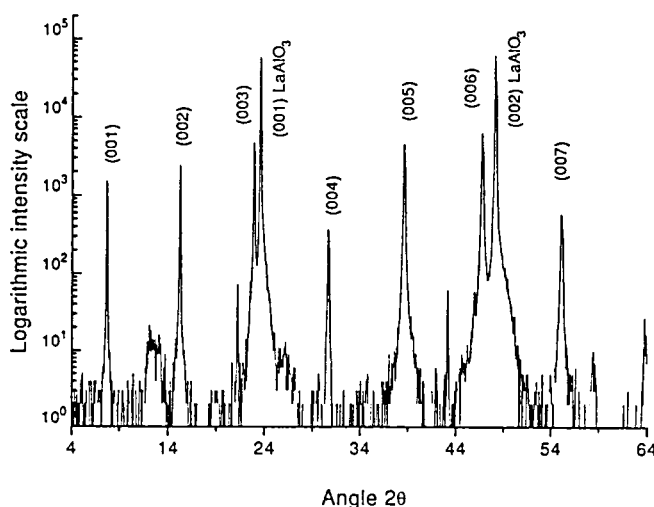


Fig. 4. A typical x-ray pattern for a film from series 1.  $T_c = 89.6$  K,  $j_c = 2 \times 10^6$  A/cm<sup>2</sup>.

The elemental composition of the films determined from EDAX measurements was approximately constant and the average metal content was in the ratio Y : Ba : Cu = 1.14 : 1.57 : 3.00, indicating that Ba-deficient films were grown.

Rocking curve measurements of the (005) peaks performed for both series of films showed that their half-widths did not exceed  $\Delta\omega = 0.6^\circ$ . The best films exhibited a small mosaic spread,  $\Delta\omega \sim 0.20^\circ$  [8]. In Fig. 5 the dependence of  $\Delta\omega$  as a function of  $p(\text{O}_2)$  is shown. Clearly a rapid narrowing in the line-width occurs when the oxygen pressure rises above  $\sim 150$  mTorr. This behaviour indicates a sensitivity of the film structure to the oxygen partial pressure and very likely corresponds to the isotherm  $T_h = 820^\circ\text{C}$  crossing the stability line in the YBCO phase diagram [5], see also Fig. 1. For  $p > 200$  mTorr, the mosaic spread in the films was roughly constant.

The growth carried out above the stability line results in a marked improvement of the superconducting parameters. While the changes in  $T_c$  are small ( $\sim 2$  K), the critical current density rises almost by a factor of 3 with an increase of the oxygen pressure from 150 to 200 mTorr. A further increase of the oxygen pressure to 300 mTorr leads to added improvement of the film structure ( $\Delta\omega = 0.22^\circ$ ), but simultaneously the decrease of critical current, apparently due to a reduction of the number of flux pinning sites.

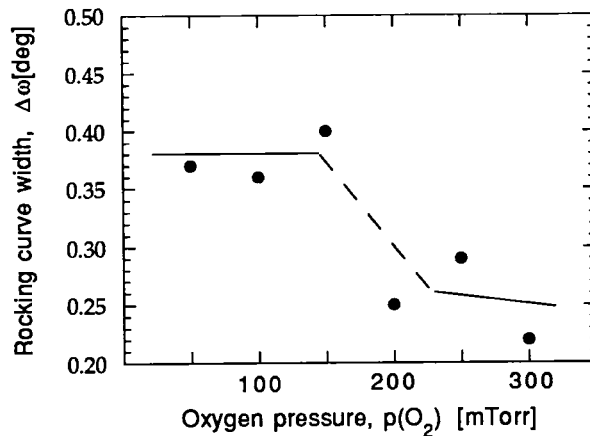


Fig. 5. Rocking curve width of the (005) x-ray reflections plotted against oxygen pressure in the deposition system during film growth,  $T_h = 820^\circ\text{C}$ .

In series 2 the mosaic spread was constant at  $\Delta\omega = 0.25^\circ \pm 0.03^\circ$ . This value is very close to that observed in film series 1 which were grown above the stability line ( $p(\text{O}_2) > 150$  mTorr). The maximum in  $j_c$  for film series 2 appeared at  $T_h = 760\text{-}770^\circ\text{C}$ , see Fig. 3. Since the mosaic spread was nearly constant in series 2, one can argue that the variations in  $j_c$  were caused by changes in the film cation-composition. The critical current density  $j_c$  has been found to be a very sensitive function of the film-cation composition [1]. Very small variations ( $\pm 0.01\text{-}0.02$ ) in the Cu content (metallic fraction  $\text{Cu}/(\text{Y} + \text{Ba} + \text{Cu})$ ) resulted in a 5 fold decrease of  $j_c$  [1]. Our EDAX measurements for the films of series 2

showed, in fact, small systematic variations in the Cu/(Y + Ba + Cu) and Ba/Y ratios. They were found to change from 0.51 to 0.54 and from 1.32 to 1.41, respectively. It is therefore possible that variations in the measured cation concentrations may account for a constant width of the rocking curves and for the simultaneous occurrence of a maximum in  $j_c$  at 760-770°C, Fig. 2. Contrary to the behaviour of  $j_c$  the critical temperature is a much weaker function of the Cu content [1]. A more extensive discussion of the effect of changes in metal composition on the structural and superconducting properties of YBCO films will be presented elsewhere [9].

In film series 1 the c-axis length was observed to correlate directly with the oxygen partial pressure, indicating a linear shortening of the c-axis with increasing oxygen partial pressure. It changes from  $c=11.75 \text{ \AA}$  (at 50 mTorr) to  $11.66 \pm 0.01 \text{ \AA}$ , (at 200 mTorr), Fig. 6. For pressures  $p > 200 \text{ mTorr}$  the c-axis length remains approximately constant.

In film series 2, changes in  $T_h$  had a rather limited effect on the c-axis length up to 800°C. As can be seen in Fig. 7 a small shortening of the c-axis length ( $\sim 0.02 \text{ \AA}$ ) occurred in the temperature range from 740 to 800°C. The Raman measurements on films of series 2 showed that the O(4) vibration frequency changed very little from  $500 \text{ cm}^{-1}$  (at 740 °C) to  $503\text{-}504 \text{ cm}^{-1}$  (at 780-800°C). These results also indicate that varying  $T_h$  from 740 to 800K changes the oxygenation of the films insignificantly [10]. The frequency range of the O(4) vibrations ( $\geq 500 \text{ cm}^{-1}$ ) indicates that the films grown below 800°C were practically fully oxygenated, that is the oxygen content was  $\geq 6.9$  [10]. Above 800 °C, an elongation of the c-axis length seems to occur, likely because of a smaller oxygen uptake at this temperature and this pressure (in the vicinity of the stability line). Indeed Raman measurements showed a small decrease of the O(4) vibration frequency from  $\sim 504 \text{ cm}^{-1}$  in films grown at 780°C to  $500 \text{ cm}^{-1}$  in those grown at 820°C, which may indicate some

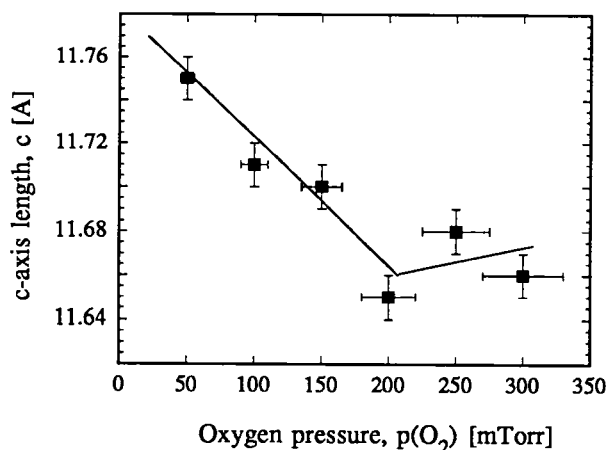


Fig. 6. C-axis parameter,  $c_0$ , as a function of the oxygen pressure during film deposition.

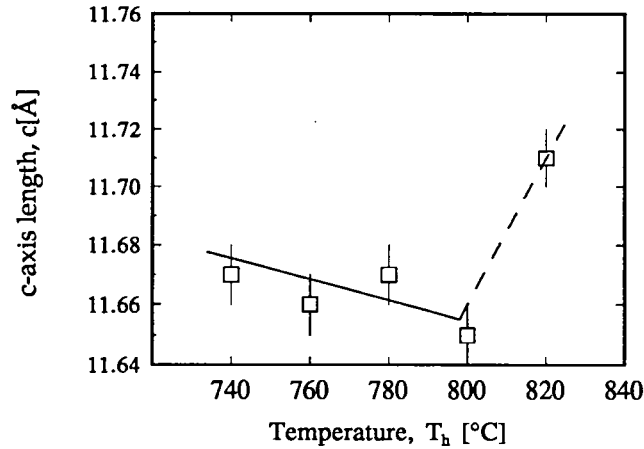


Fig. 7. C-axis parameter,  $c_0$ , as a function of the temperature of the film deposition,  $T_h$ .

oxygen loss. Fig. 8 shows that at a constant oxygen pressure of 200 mTorr, the c-axis length reaches its minimum for  $T_h$  close to 780°C ( $\pm 20^\circ\text{C}$ ) yielding  $c = 11.66 \pm 0.01 \text{ \AA}$ .

Close correlations have also been observed between the c-axis length and the  $T_c$  and  $j_c$  parameters in the films grown in series 1 and 2. Maxima in both  $T_c$  and  $j_c$  appear when the lattice parameter  $c_0 = 11.66\text{-}11.68 \text{ \AA}$ , see Fig. 8 and 9. In film series 1 (variable oxygen pressure)  $T_c$  apparently passes through a maximum as a function of  $c_0$  whose value changes due to the change in oxygen content. A decrease of  $T_c$  by  $\sim 1\text{K}$  seems to occur for the highest pressure (300 mTorr). This observation seems to be in agreement with other reports [11], showing that the maximum of  $T_c$  in  $\text{Y}_1\text{Ba}_2\text{Cu}_3\text{O}_z$  takes place for the oxygen content  $z = 6.93 (\pm 0.02)$ , not  $z = 7.00$ . The dependence of  $T_c$  versus c-axis length presented in Fig. 9 can be approximated by a quadratic function, which is very similar to

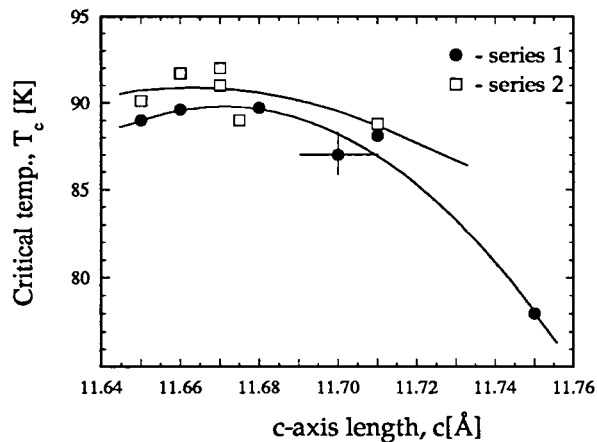


Fig. 8. Critical temperature  $T_c$  of the YBCO films grown at a constant oxygen pressure (open squares) and constant temperature (black circles) as a function of the lattice parameter  $c_0$ .



that illustrating the dependence of  $T_c$  on hole concentration ( $h^+$ ) per  $\text{CuO}_2$  plane, induced either by chemical substitutions [12] or the oxygen content [13, 14].

The films from series 2 (variable  $T_h$ ) exhibited relatively small changes in  $c_0$  which is consistent with small variations in  $T_c$  ( $\sim 2\text{K}$ ), see Fig.8. These changes in  $T_c$  due to variations in  $c_0$  are very likely caused by small systematic changes in the film cation composition as discussed above. However, the critical current density is very sensitive even those small changes in  $c_0$ , see Fig.9. This observation is in agreement with other reports [1] and will be discussed in detail elsewhere [9].

The EDAX measurements showed that the shortest  $c_0$  occurred for Ba-deficient, but Y-rich films. The highest values of  $T_c$  and  $j_c$  were observed in off-stoichiometric (Ba-deficient, Y rich) films ( $\text{Y}_{1+x}\text{Ba}_{2-y}\text{Cu}_3\text{O}_z$ ;  $x = 0.11-0.18$ ,  $y = 0.32-0.43$ ). This observation is in good agreement with a Stanford group report [15], where the Ba/Y ratio for the highest  $T_c$  was observed to be about 1.4. This value is almost identical with that found in our EDAX measurements ( $\text{Ba}/\text{Y} = 1.61/1.15 = 1.4$ ). The Stanford group [15]

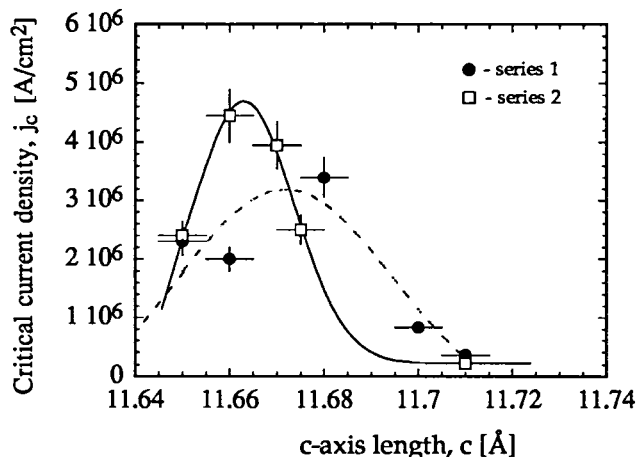


Fig. 9. Critical current density  $j_c$  in the YBCO films grown at a constant oxygen pressure (open squares) and constant temperature (black circles) as a function of the lattice parameter  $c_0$ .

also found that a large number of Y for Ba substitutions resulted in a significant presence of point defects which act as effective flux pinning centres [16]. Also Y for Ba substitutions may lead to some shortening of the c-axis length. In our fully oxygenated films, the c-axis length is 11.66 Å, as compared to the ideal value of 11.6802 Å [13].

#### 4. Conclusions

Application of two different deposition protocols enabled us to explore regions in the phase diagram (oxygen pressure  $p(\text{O}_2)$  vs. growth temperature ( $T_h$ ) of YBCO films

situated close to its stability line. The films with the best structure were grown above and to the right of the stability line, i.e. toward the interior of the stability region for YBCO, and those films also exhibited the highest critical temperature  $T_C$ . In contrast the highest  $j_C$  (up to  $4.5 \times 10^6$  A/cm<sup>2</sup>) occurred in films grown in the vicinity of the stability line, where  $T_C$  was 1-2 K lower than the maximum value observed in this work. These results indicate that our best epitaxial films approach the structural quality of single crystals where the critical current density is low because of reduced density of flux pinning sites.

It is thus clear that the best conditions for optimum  $T_C$  do not result in samples with the highest  $j_C$ . The fabrication of films with both high  $T_C$  and  $j_C$  therefore requires some sort of compromise between structural perfection (high  $T_C$ ) and the presence of crystallographic defects (high  $j_C$ ).

## Acknowledgments

The financial support of National Science and Engineering Council of Canada (NSERC), Industry Canada (STP-AIM Program), BC Ministry of Employment and Investment, and Furukawa Electric Co., is gratefully acknowledged.

## References

- [1] N.G. Chew, S.W. Goodyear, J.A. Edwards, J.S. Satchell, S.E. Blenkinsop, and R.G. Humphreys, *Appl. Phys. Lett.* **57**, 2016(1990).
- [2] R. Feenstra, T.B. Lindemer, J.D. Budai, and M.D. Galloway, *J. Appl. Phys.* **69**, 6569(1991).
- [3] R. Bormann and J. Noelting, *Appl. Phys. Lett.*, **54**, 2150(1989).
- [4] R. Hammond and R. Bormann, *Physica C* **162-164**, 703(1989).
- [5] R. Beyers and B.T. Ahn, *Annu. Rev. Mater. Sci.* **21**, 335(1991)
- [6] W.B. Xing, B. Heinrich, J. Chrzanowski, J.C. Irwin, H. Zhou, A. Cragg and A.A. Fife, *Physica C* **205**, 311(1993).
- [7] C. Thomsen, and R. Wegerer, H.-U. Habermeier and M. Cardona, *Sol. St. Commun.* **83**, 199(1992).
- [8] J. Chrzanowski et al, this conference.
- [9] J. Chrzanowski et al., to be published.
- [10] R. M. Macfarlane, H.J. Rosen, E.M. Engler, R.D. Jacowitz, and V.Y. Lee, *Phys. Rev. B* **38**, 284(1988).
- [11] A. Altendorf, X.K. Chen, J.C. Irwin, R. Liang and W.N. Hardy, *Phys. Rev. B* **47**, 8140(1993).
- [12] J. J. Neumeier and H. A. Zimmermann, *Phys. Rev. B* **47**, 8385(1993).
- [13] J.D. Jorgensen, B.W. Veal, A.P. Paulikas, L.J. Nowicki, G.W. Crabtree, H. Claus, and W.K. Kwok, *Phys. Rev. B* **41**, 1863(1990).
- [14] e.g. J.L. Tallon and G.V.M. Williams, *J. Less- Common. Metals* **164 & 165**, 70(1990), and references cited therein.
- [15] V. Matijasevic, P. Rosenthal, K. Shinohara, A.F. Marshal, R.H. Hammond, and M.R. Beasley, *J. Mater. Res.* **6**, 682(1991).
- [16] T.L. Hylton, and M.R. Beasley, *Phys. Rev. B* **41**, 11669(1990).